Unravelling the mystery of fish scales in lowering ice adhesion

Journal:	*SCIENCE CHINA Materials*
Manuscript ID	SCMs-2024-0018.R1
Manuscript Type:	Article
Date Submitted by the Author:	08-Feb-2024
Complete List of Authors:	Wang, Feng; Suzhou Laboratory, Liu, Siqi; Norwegian University of Science and Technology Xiao, Senbo; Norwegian University of Science and Technology Skallerud, Bjørn ; Norwegian University of Science and Technology Zhang, Zhiliang; Norwegian University of Science and Technology, ; NTNU He, Jianying; Norwegian University of Science and Technology
Keywords:	anti-icing, fish scale, ice adhesion, dynamic behaviors, sequential rupture
Speciality:	Structural Materials
Note: The following files were submitted by the author for peer review, but cannot be converted to PDF. You must view these files (e.g. movies) online.	
Movie S1.mp4	

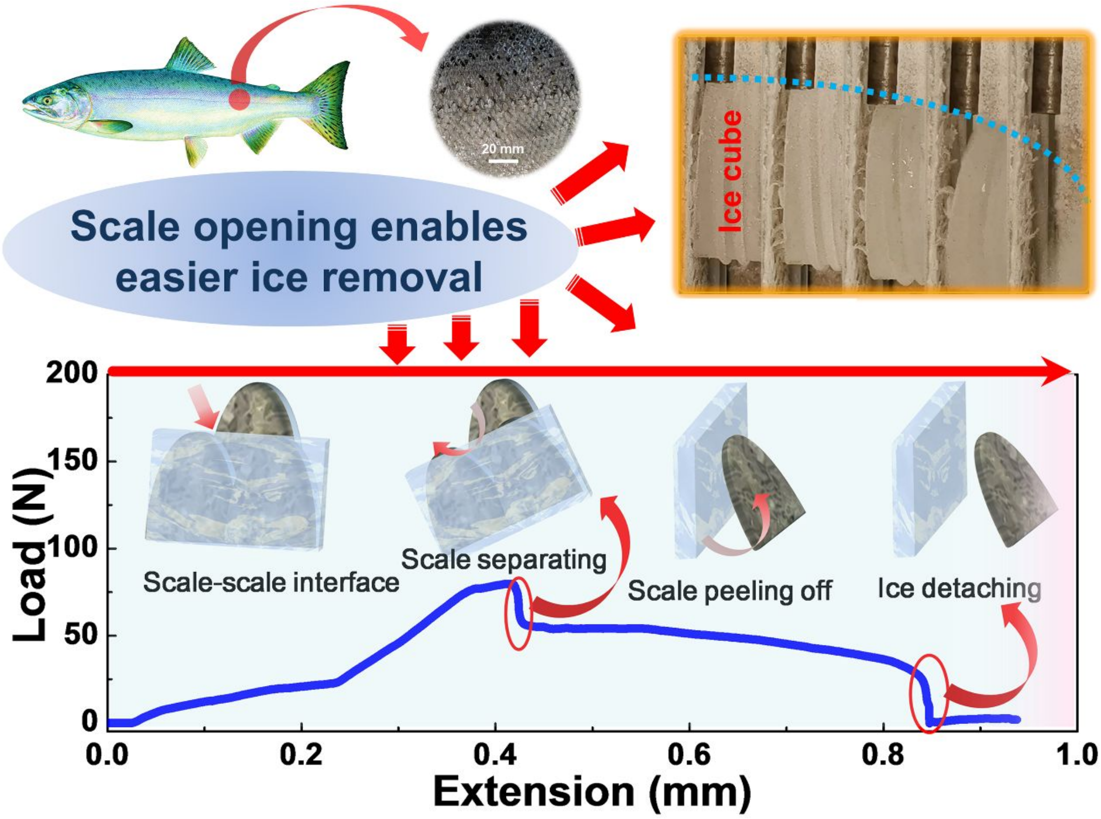
Scale opening enables easier ice removal
20 mm
Ice cube
Scale-scale interface
Scale separating
Scale peeling off
Ice detaching
Load (N)
Extension (mm)
200
150
100
50
0
0.0
0.2
0.4
0.6
0.8
1.0

Unravelling the mystery of fish scales in lowering ice adhesion

Feng Wang[a, b], Siqi Liu[a], Senbo Xiao [a], Bjørn Skallerud [a], Zhiliang Zhang[a, *], and Jianying He[a, *]

a. Department of Structural Engineering, Norwegian University of Science and Technology (NTNU), Trondheim 7491, Norway.

b. Suzhou Laboratory, Suzhou 215000, China.

*E-mail: zhiliang.zhang@ntnu.no, jianying.he@ntnu.no

Abstract

The influence of static surface properties, such as free energy, toughness, and elasticity, on icephobicity has been extensively researched and documented in existing literature. However, there remains a limited understanding of the role played by surface dynamic characteristics in facilitating ice removal. This study investigates the ice adhesion strength of authentic Arctic salmon (Salmon salar) skin, revealing intriguing anisotropic ice adhesion behavior. Results indicate a significant decrease in ice adhesion strength (141 ± 47 kPa) when sheared against the growth orientation of fish scales compared to shearing along this orientation (353 ± 95 kPa). The distinctive structural evolution of fish scales during shearing can lead to a sequential rupture process, thereby diminishing ice adhesion. Additionally, the study highlights the significance of the opening and peeling capacity of fish scales in controlling ice detachment, defined as the ability of unit scales to separate from their underlying structures and adhesives under applied force. Enhancing this capacity could further

reduce ice adhesion strength (66 ± 15 kPa), facilitating effortless ice detachment on fish scales. The mechanical robustness of fish scales offers new possibilities for designing hard and durable anti-icing surfaces.

Keywords: fish scale, ice adhesion, dynamic behaviors, sequential rupture, anti-icing.

Introduction

Icing is a phenomenon commonly observed in nature (1). Excessive ice accumulation on infrastructure, transport facilities, and renewable energy production equipment has resulted in numerous safety and economic problems (2–6). Passive anti-icing surfaces that enable easy ice removal without active chemical/energy input have received worldwide attention as a mitigation method (7-9). Anti-icing surfaces are typically designed to repel water, delay ice nucleation, reduce frost formation and coverage, and lower ice adhesion (7–12). However, if surfaces are exposed to air for a prolonged period of time at low temperatures, ice will eventually form in areas where water cannot be drained, such as on standstill wind turbine blades. Lowering ice adhesion and removing ice automatically under wind and gravitational force has become a desirable strategy (13–18).

Cutting-edge icephobic surfaces with minimal ice adhesion primarily rely on manipulating static surface parameters. Ice adhesion strength (τice) on solid surfaces is commonly described using a semi-empirical equation: $\tau_{ice} = \sqrt{E^* G/\pi a \Lambda}$,where $E*$ represents the surface's elastic modulus, G denotes surface free energy, a signifies the length of interface cracks, and Λ is a non-dimensional constant (19, 20). Adjusting static surface parameters, such as surface free energy and elastic modulus, can effectively reduce surface ice adhesion (7, 9, 21, 22). Silicone elastomers, characterized by low surface energy and elastic modulus, are frequently employed as icephobic surfaces (9, 14, 15, 23, 24). Interfacial toughness is another parameter utilized to modify surface ice adhesion (13, 25, 26). Surfaces with low interfacial toughness require nearly the same mechanical force for ice removal on surfaces larger than a certain size (13, 27). While static strategies have shown remarkable icephobicity on soft gels and rubbers, designing anti-icing surfaces for hard materials remains challenging. A prevalent approach to reducing ice adhesion on hard surfaces is employing a superhydrophobic structure with low $E*$ and large a. However, the practical applications of superhydrophobic surfaces are hindered by their poor durability in icing/de-icing cycles. Achieving durable low ice adhesion on high modulus surfaces remains a significant challenge.

State-of-the-art icephobic surfaces with low ice adhesion are primarily designed by manipulating static surface parameters. To describe ice adhesion strength (τice) on solid surfaces, a semi-empirical equation, $\tau_{ice} = \sqrt{E^* G/\pi a \Lambda}$, is commonly used. $E*$ represents the elastic modulus of the surface, G represents the surface free energy, a represents the length of interface cracks, and Λ is a non-dimensional constant (19, 20). According to this theory, adjusting static surface parameters such as surface free energy and surface elastic modulus can decrease surface ice adhesion (7, 9, 21, 22). For example, silicone elastomers with low surface energy and elastic modulus are a common type of icephobic surface (9, 14, 15, 23, 24). Another parameter, interfacial toughness, has also been used to modify surface ice adhesion (13, 25, 26). The surfaces with low interfacial toughness allow for the use of nearly the same mechanical force to remove ice on surfaces larger than a certain size (13, 27). While static strategies have achieved excellent icephobicity on soft gels and rubbers, designing anti-icing surfaces on hard materials remains a challenge. A common approach to reducing ice adhesion on hard surfaces is to use a superhydrophobic structure with low E^* and large a. However, the practical applications of superhydrophobic surfaces are limited due to their poor durability in icing/de-icing cycles. Achieving durable low ice adhesion on high modulus surfaces remains a significant challenge.

Recent studies have highlighted the potential of leveraging dynamic properties in both artificial and bioinspired surfaces to enhance the design of ice-repellent surfaces (8, 16, 18, 24, 28). The modulation of surface properties in response to temperature, light, and mechanical stimuli can be harnessed to create surfaces with exceptionally low ice adhesion strength (29–31). Golovin et al. conducted a notable study demonstrating that the dynamic buckling behavior of metallic surfaces can significantly mitigate ice adhesion (32). Thus, utilizing the dynamic nature of surface properties presents a promising strategy for reducing ice adhesion on hard surfaces with improved mechanical robustness.

Fish scales, renowned for their distinctive wettability, have spurred the development of subaquatic, low-adhesion superoleophobic surfaces (33, 34). Yet, our understanding of ice adhesion on fish scales remains limited (35). In our prior research employing atomistic modeling, fish scale-like structures revealed a distinctive sequential rupture mechanism that mitigates ice adhesion. Norwegian salmon, an anadromous species abundant in Norway's seas and rivers, ranks among the world's most consumed fish. While anti-icing characteristics are irrelevant to salmon, unraveling how fish scales reduce ice adhesion could foster innovative anti-icing strategies, particularly in Arctic regions. This study delved into the de-icing dynamics of authentic salmon skin, altering de-icing directions relative to scale orientation to gauge varied ice adhesion strengths. Findings underscore the correlation between ice adhesion strength and the mode of rupture at ice-surface contact points. Detailed observation of ice removal from fish scales elucidated the underlying mechanisms, highlighting the pivotal role of scales' opening and peeling in mitigating adhesion during de-icing. Modulating surface structure parameters to enhance scales' opening or peeling capability holds promise for reducing ice adhesion. Therefore, fish scales inspire a new principle for fabricating robust surfaces with low ice adhesion.

Results and discussions

This work investigates the adhesion of ice on authentic salmon skin. Figure 1a illustrates the structures of fish scales on Atlantic salmon skin, characterized by their specific orientation. Surface analysis indicates that fish scales exhibit a rough texture composed of ribbing micropatterns. Previous research has highlighted the remarkable underwater superoleophobic properties of fish scales, attributed to their superhydrophilicity and micropatterned structure (33, 34). These properties prevent oil and fouling contamination, facilitating exceptional self-cleaning abilities (33). Additionally, fish scales exhibit intriguing mechanical characteristics, such as flexibility, high strength, resistance to penetration, and lightweight nature [36]. However, the potential anti-icing properties of fish scales remain unexplored. Mechanical testing of fish scales depicted in Figure 1b was conducted using cylindrical flat punch nanoindentation (see Supplementary Section 1) (37). Fish scales demonstrate greater durability compared to elastomers. According to the adhesion equation $\tau_{ice} = \sqrt{E^* G/\pi a \Lambda}$, materials with low surface energy and elastic modulus, such as plastics and rubbers, typically exhibit lower ice adhesion than metals and ceramics (Figure 1c). Consequently, state-of-the-art anti-icing surfaces primarily utilize soft polymers (8, 9). Nonetheless, enhancing the mechanical and chemical durability of soft materials poses a significant challenge in achieving prolonged icephobicity (8, 9). Despite its high elastic modulus, ice adhesion strength on fish scales is significantly lower than on many plastics and rubbers. Further exploration of the role of fish scales in mitigating ice adhesion holds promise for developing robust and enduring anti-icing surfaces.

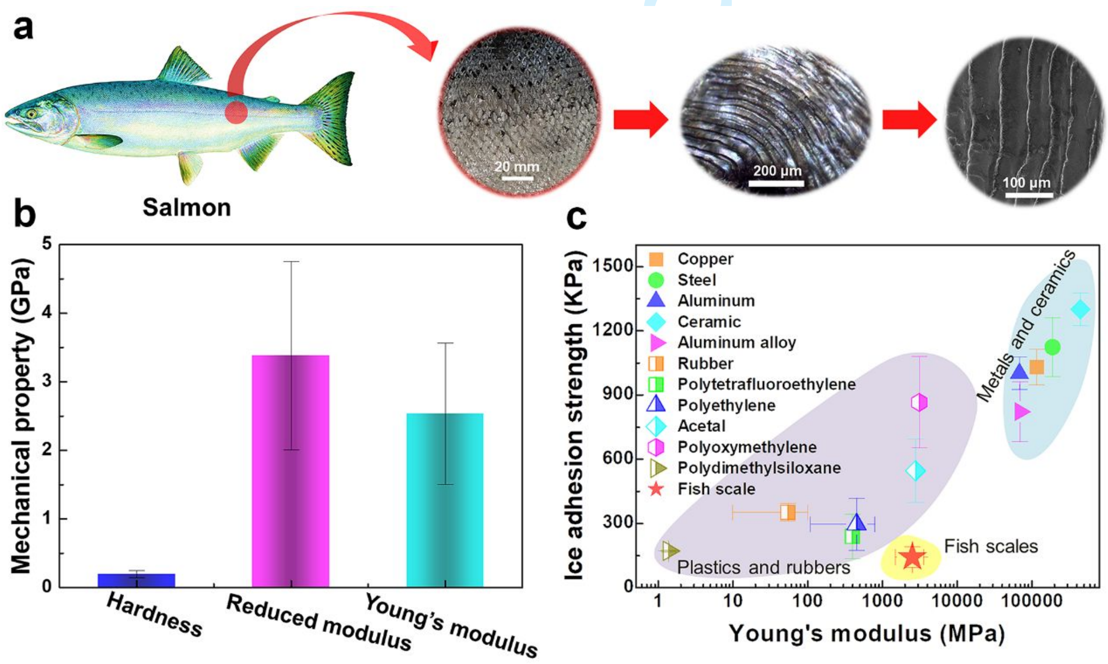

Figure 1. Properties of a real salmon scale. (a) The appearance of fish scales, observed using a camera, an optical microscope and a scanning electron microscope (SEM). (b) Nanoindentation is used to determine the mechanical characteristics of fish scales. (c) The ice adhesion strength on various surfaces and is comparable to the ice adhesion strength on fish scales. The ice adhesion strength on copper, steel, aluminum, ceramic, aluminum alloy, and rubber is obtained from Ref. 38 (38). The ice adhesion strength of polytetrafluoroethylene, polyethylene, acetal, and polyoxymethylene is obtained from Ref. 39 (39). The Young's modulus of the various materials is obtained from Ref. 39 (39). Ref. 40 (40) reports on the ice adhesion strength of polydimethylsiloxane as well as the Young's modulus. The ice adhesion strength on the fish scale is determined by de-icing against the scale growth orientation.

The ice adhesion strength on fish scales exhibits anisotropy, depending on the direction of the applied shearing force (Fig. 2a). A comparative analysis was conducted to assess the ice adhesion strength on fish scales during de-icing along ($F_{0°}$) and against ($F_{180°}$) the scale growth orientation (Fig. 2b). The measured ice adhesion by $F_{180°}$ is 141 ± 47 kPa, representing a reduction of up to 60% compared to F0° (353 ± 95 kPa). Examination of the load-extension curves for both de-icing directions allows for the discussion of the underlying mechanism. Figure 2c illustrates a typical load-extension curve when applying a shearing force along the scale growth orientation, reaching maximum load and swiftly decreasing to zero (20). The robust mechanical interlocking between ice and rough fish scales necessitates significant force for ice removal. Upon detachment of the ice cube from fish scales (Fig. 2c), the surface appears rough, indicating strong interlocking during ice formation. Conversely, applying a shearing force against the scale growth orientation results in a distinctive curve, where the load gradually evolves before decreasing to zero (Fig. 2d). Our prior research, employing atomistic modeling and molecular dynamics simulation, identified two distinct fracture modes responsible for this phenomenon (35). Ice removal along the scale orientation leads to simultaneous rupture of the entire scale-ice interface, termed concurrent rupture mode. Conversely, de-icing against the scale orientation follows a sequential rupture mode, where the interface breaks incrementally. It has been suggested that the sequential rupture mode can result in elongated energy depth and, consequently, a significantly lower rupture force compared to the concurrent rupture mode (35). However, experimental clarification and understanding of these differences are lacking. This study demonstrates the reduced ice adhesion on fish scales through de-icing against the scale growth orientation, validating the role of sequential rupture in diminishing ice adhesion strength.

Figure 2d illustrates the dynamic fracture occurring during de-icing against the orientation of scale growth. This process comprises three stages: scale opening, scale peeling, and ice detachment. Initially, the force increases until the scale-scale interfaces fracture, initiating scale opening. Upon reaching maximum load, the interactions between scales are disrupted. Consequently, the force required to displace the ice decreases slightly, although the ice remains adhered to the surface. The process of rupturing fish scales is governed by peeling them from the ice due to their flexibility. Peeling the scales necessitates a smaller shearing force compared to fracturing the scale-scale interfaces. The load gradually diminishes during scale peeling and diminishes to zero as the ice detaches.

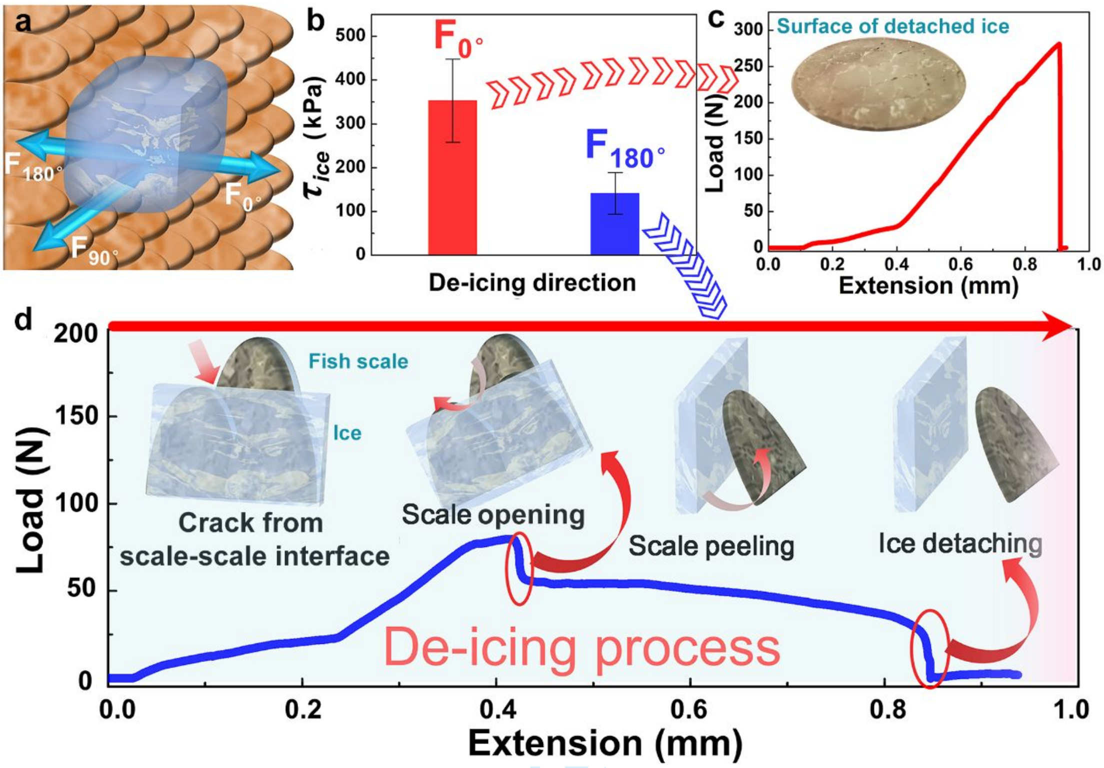

Figure 2. Ice adhesion behaviors on salmon scales. (a) A schematic graphic depicts the direction of the shearing force used during the de-icing operation. $F_{0°}$, $F_{90°}$, and $F_{180°}$ are the de-icing forces along, vertical to, and against the direction of fish scale growth, respectively. (b) Ice adhesion strength on fish scales through de-icing along and against the direction of fish scale expansion. (c) The load-displacement curve for de-icing along the direction of fish scale growth. (d) The load-displacement curve and dynamic evolution of scales and ice during de-icing are plotted against the direction of fish scale growth.

Based on the preceding discussion, it becomes apparent that the opening of fish scales during the de-icing process is paramount for achieving minimal ice adhesion. To elucidate the impact of opening capacity, inversely linked to scale-scale adhesion, on reducing ice adhesion, we conducted an analysis of fish scales with varying sizes, as delineated in Supplementary Section 2. Figure 3a illustrates three distinct types of fish scales, each measuring 5.54 mm, 4.64 mm, and 3.53 mm, sourced from the skin of Atlantic salmon. Ice adhesion strength post-de-icing in the $F_{0°}$, $F_{90°}$, and $F_{180°}$ directions is detailed in Figure 3b. Notably, discernible trends emerge in de-icing with $F_{0°}$ and $F_{90°}$ in contrast to de-icing along the $F_{180°}$ direction. Ice adhesion diminishes as the scale size decreases during de-icing with $F_{0°}$ and $F_{90°}$. However, de-icing against the direction of scale growth results in increased ice adhesion strength as the scale size decreases. This variation arises from different fracture modes influencing ice adhesion across scale sizes. Reducing the scale size diminishes surface roughness, thereby mitigating mechanical interlocking between ice and the surface. Consequently, during de-icing at $F_{0°}$ and $F_{90°}$ without dynamic surface changes or with slight surface opening, ice adhesion strength is lower on surfaces with smaller scales. However, reducing the scale size enhances the threshold of scale opening.

As illustrated in Fig. 3c, a simplified model depicting the adhesion between scales is presented. Each fish scale overlaps with two others beneath it. In freezing conditions, water between the scales freezes, binding them together. To diminish ice adhesion and facilitate scale opening, it's vital to induce a fracture where the scales adhere. Consequently, ice adhesion strength is inversely proportional to the scale's opening capacity. Reducing the scale size enlarges the adhesion area between the scale and the ice cube, diminishing the scale's opening capacity and necessitating greater forces. When de-icing along the $F_{180°}$ direction, decreasing the scale size diminishes the scale's opening capacity, resulting in stronger ice adhesion. With a scale size of 3.53 mm, ice adhesion on fish scales during de-icing at $F_{0°}$ and $F_{90°}$ mirrors that at $F_{180°}$, indicating negligible differences in scale opening capacity for this size. An alternative method to modulate the scale's opening capacity is by adjusting the water content. After a year in the freezer, the scales maintained their shape with reduced water content due to ice sublimation. Lower water content weakens scale-scale interactions after freezing, enhancing the scale's opening capacity. This facilitates easier separation between scales. The results in Fig. 3b demonstrate that ice adhesion strength on fish scales with reduced water content during de-icing along $F_{180°}$ is only 66 ± 15 kPa, falling within the range of icephobic surfaces. Enhancing the opening capacity of fish scale-like structures can effectively mitigate surface icephobicity.

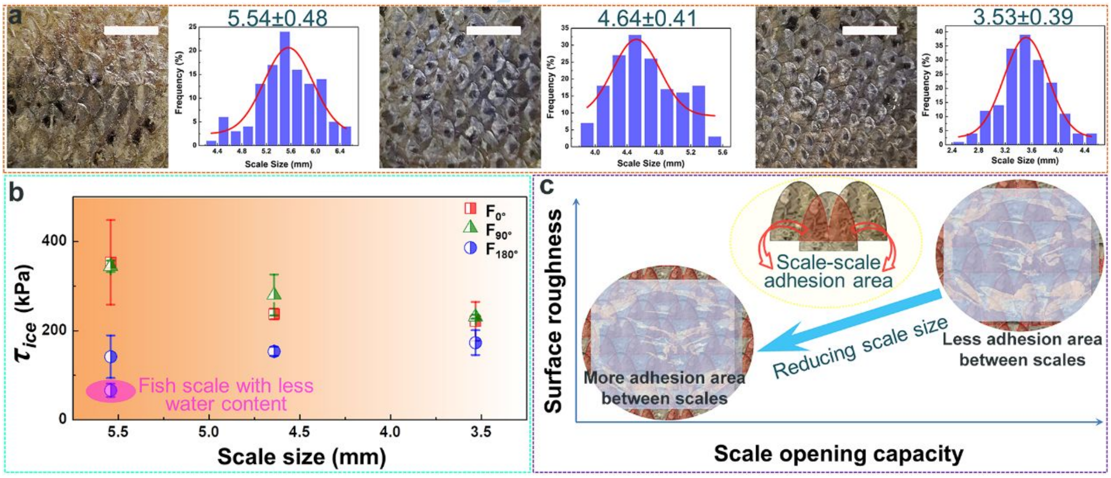

Figure 3. Ice adhesion behaviors on fish scales with different sizes. (a) Fish scales of various sizes are used to measure ice adhesion strength. Each variety of fish skin had at least 100 scales measured to determine its size. The photos' scale bars are 10 mm. (b) The ice adhesion strength through de-icing in $F_{0°}$, $F_{90°}$, and $F_{180°}$ directions on surfaces of different scale sizes. (c) A schematic figure depicts the effect of scale size on surface roughness and scale opening capacity.

After the fish scales have opened, ice fracture is governed by the peeling process. Supplementary Movies S1 and S4 provide detailed documentation of de-icing against the fish scale growth orientation and the peeling process. As illustrated in Fig. 4a, fish scales exhibit various bending patterns during de-icing. Importantly, the scales revert to their original states immediately after ice detachment. Designing scales with mechanical robustness can confer durable icephobicity through fish scale-like structures. These scales can retain their shape and functionality during icing and de-icing cycles on actual fish skin. Nonetheless, weak connections between the scales and skin pose a problem, as the scales are prone to being dislodged from the fish skin when removing ice. Enhancing the interaction between scales and substrate is a critical endeavor for the future design of fish scale-inspired anti-icing surfaces

Peeling an elastic film from a rigid substrate can generally be described by Eq. 1 (*41*)

$$\left(\frac{F}{b}\right)^2 \frac{1}{2Ed} + \left(\frac{F}{b}\right)(1 - cos\theta) - R = 0 \qquad (1)$$

The formula for calculating the applied peeling force (F) encompasses several parameters, including the width of the adhesive (b), adhesive thickness (d), Young's modulus of the film (E), peeling angle (θ), and adhesive energy (R). A schematic diagram illustrating these parameters is available in Supplementary Section 4. During fish scale de-icing, the scales are treated as elastic films, and the ice as a rigid substrate. The angle θ (= 180° - β) can be determined as depicted in Figure 4b-d. Although scales exhibit various bending behaviors, β values consistently decrease from approximately 135° to 30°. Consequently, the θ in the scale peeling process increases from about 45° to 150°. Meanwhile, the force required for ice removal gradually decreases until detachment. It's worth noting that the scales' bending response affects angle α, not angle β at detachment (Fig. 4b-d). Scale peeling capacity depends on intrinsic parameters such as R, E, d, and b of fish scales. De-icing forces on scales with reduced water content (Supplementary Fig. S6) show significantly lower peeling forces due to reduced R compared to those in Fig. 2d. Future research focusing on modulating R, E, d, or b and understanding their relationships with scale peeling capacity could facilitate easier ice removal from fish scale-like surfaces.

The connection between scales and skin must be considered, as it can impact the de-icing process. A soft, mechanically friction-free connection between scales and skin can facilitate crack formation at scale-scale interfaces compared to a hard connection. Additionally, a soft connection can benefit scale opening, emphasizing the importance of using soft salmon skin to reduce ice adhesion on scales. Based on the preceding discussions, it's evident that the sequential rupture mode in de-icing against fish scale growth orientation can lead to exceptionally low ice adhesion. The critical parameters controlling ice removal are scale opening capacity and scale peeling capacity. Enhancing these parameters can facilitate easy ice detachment. Fish scale-inspired surfaces with improved scale opening and peeling capacity hold promise for future anti-icing applications.

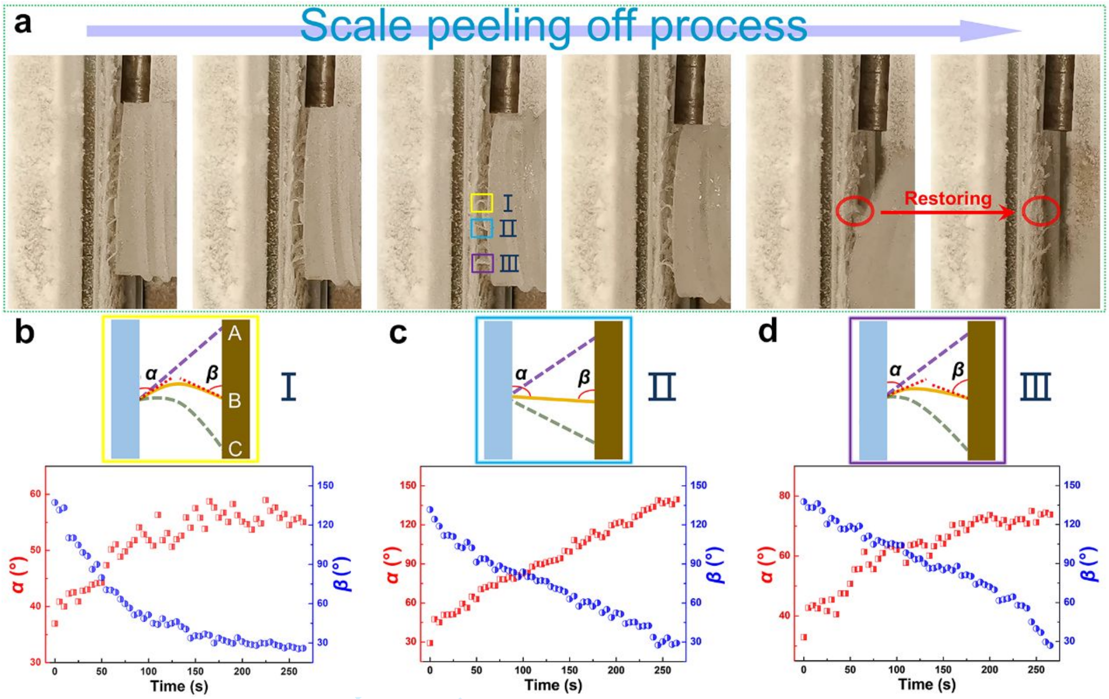

Figure 4. Fish scale peeling behaviors in de-icing. (a) The photographs depict the fish scales peeling off process as captured by a camera. The angles of the fish scale to the skin and ice change during the de-icing process. Figures (b), (c), and (d) show the angle evolutions of three typical scales (Ⅰ, Ⅱ, and Ⅲ) over de-icing time.

Conclusions

This work investigates anisotropic ice adhesion behaviors by examining the ice adhesion strength on Arctic salmon skin. Shearing against the fish scale's growth direction yields a 60% reduction in ice adhesion strength (141 ± 47 kPa) compared to shearing along the growth orientation (353 ± 95 kPa). This diminished adhesion is attributed to the dynamic response of fish scales when sheared against their growth orientation. The de-icing process follows a sequential rupture mode, with fish scales opening first and then gradually peeling off. The scale opening and peeling capacity are identified as critical parameters controlling ice detachment. Enhancing these parameters can lead to further reductions in ice adhesion strength (66 ± 15 kPa). Despite bending during de-icing, fish scales regain their initial shape post-ice removal. Additionally, the high Young's modulus and mechanical/chemical robustness of fish scales contribute to their effectiveness as durable anti-icing surfaces. Thus, the mechanism by which fish scales mitigate ice adhesion presents opportunities for designing effective icephobic surfaces. Developing structures inspired by fish scales and dynamic response surfaces holds promise for future anti-icing research.

Materials and methods

Materials

For the tests, a piece of fish skin from an Arctic Salmon purchased from Ravnkloa Fish & Shellfish AS in Trondheim, Norway, was used. The fish skin is cut into small pieces measuring 50 mm × 50 mm and adhered to a glass substrate (60 mm × 60 mm) for ice adhesion testing. Prior to adhesion, the underside of the skin is dried with wipers several times. The fish skin is then firmly attached to the glass using Lynlim (Scotch, 3M Norge AS). Different parts of the fish skin produce scales of varying sizes. For instance, the skin near the fishtail has smaller scales than the skin near the fishhead. The fabricated samples were stored in a freezer at -18°C for subsequent ice adhesion tests.

Characterizations

The morphology of fish scales was characterized using a combination of a camera, DIC microscope (Zeiss AxioScope A1 for reflected light, BF-DIC/POL, Carl Zeiss), and a field-emission scanning electron microscope (FEI APREO SEM). Direct observation of the scales was conducted without any additional treatment using the camera and optical microscope. Prior to SEM analysis, the scales underwent drying in an oven at

60°C for 24 hours, followed by coating with 10 nm platinum/palladium layers using a sputter coater (208 HR B, Cressington). Ice adhesion strength was assessed utilizing a universal mechanical tester (Instron Model 5944) equipped with a custom cooling system and chamber, as detailed in previous studies. A polypropylene centrifuge tube, with a wall thickness of 1 mm and an inner diameter of 28 mm, was placed on the fish scales. Subsequently, 6 mL of deionized water was added to the mold, and the samples were stored in a freezer at -18°C for 3 hours to ensure complete ice formation. To prevent water leakage onto the fish scales, a weight of 200 g was applied to ensure tight contact between the mold and scales, sealing the contacted area with babassu oil. Before testing, the samples were transferred from the freezer to the cooling chamber of the testing machine and stabilized at -18°C for 15 minutes. During the adhesion test, a force probe propelled the adhered samples at a velocity of 0.01 mm−1, with the probe positioned within close proximity to the tested coating surface (less than 1 mm) to minimize torque on the ice cylinder. Five samples were prepared for each adhesion test type to determine the average adhesion strength. Although salmon is commonly available, tests were conducted using a single large salmon to maintain consistency. Five repeated tests were performed on intact surface samples for each adhesion measurement type to mitigate sampling differences and uncertainties. Supplementary Movie S1 depicts the de-icing process against the growth direction of fish scales, showcasing their dynamic surface properties and effectiveness in ice removal.

Competing Interests

The authors declare no conflicts of interest.

Data availability Statement

The data supporting the findings of this investigation are accessible from the corresponding author upon reasonable request.

Acknowledgments

The Norwegian Research Council is acknowledged for its support of the NANO2021 project Dual-Functional Anti-Gas Hydrate Surfaces (DAndra, 302348), the FRIPRO project Towards Design of Super-Low Ice Adhesion Surfaces (SLICE, 250990), and the Norwegian Micro- and Nano-Fabrication Facility, NorFab (295864).

References

1. K. L. Carey, Icings developed from surface water and ground water. (1973).
2. W. Zhang *et al.*, Investigation and Analysis of Icing and Snowing Disaster Happened in Hunan Power Grid in 2008. *Power System Technology* **8**, (2008).
3. W. Yu *et al.*, Icing problems on road in Da Hinggangling forest region and prevention measures. *Cold regions science and technology* **42**, 79-88 (2005).
4. F. R. Mosher, D. Schaum, C. Herbster, T. Guinn, Analysis of causes of icing conditions which contributed to the crash of continental flight 3407. (2010).
5. F. Sutherby, Icing Problems on Ships. *Journal of Glaciology* **1**, 546-548 (1951).
6. A. G. Kraj, E. L. Bibeau, Phases of icing on wind turbine blades characterized by ice accumulation. *Renewable Energy* **35**, 966-972 (2010).
7. M. J. Kreder, J. Alvarenga, P. Kim, J. Aizenberg, Design of anti-icing surfaces: smooth, textured or slippery? *Nature Reviews Materials* **1**, 1-15 (2016).
8. F. Wang *et al.*, Dynamic Anti‐Icing Surfaces (DAIS). *Advanced Science* **8**, 2101163 (2021).
9. Y. Zhuo *et al.*, Gels as emerging anti-icing materials: a mini review. *Materials Horizons* **8,** 3266-3280 (2021).
10. F. Wang *et al.*, Anti-gas hydrate surfaces: perspectives, progress and prospects. *Journal of Materials Chemistry A* **10**, 379-406 (2022).
11. R. Chatterjee, D. Beysens, S. Anand, Delaying ice and frost formation using phase‐switching liquids. *Advanced Materials* **31**, 1807812 (2019).
12. Y. Jin *et al.*, Inhibiting condensation freezing on patterned polyelectrolyte coatings. *ACS nano* **14**, 5000-5007 (2020).
13. K. Golovin, A. Dhyani, M. Thouless, A. Tuteja, Low–interfacial toughness materials for effective large-scale deicing. *Science* **364**, 371-375 (2019).
14. K. Golovin *et al.*, Designing durable icephobic surfaces. *Science advances* **2**, e1501496 (2016).
15. P. Irajizad *et al.*, Stress-localized durable icephobic surfaces. *Materials Horizons* **6**, 758-766 (2019).

16. F. Wang *et al.*, Liquid layer generators for excellent icephobicity at extremely low temperatures. *Materials Horizons* **6**, 2063-2072 (2019).

17. Y. Wang *et al.*, Organogel as durable anti-icing coatings. *Science China Materials* **58**, 559-565 (2015).

18. J. Liu *et al.*, Distinct ice patterns on solid surfaces with various wettabilities. *Proceedings of the National Academy of Sciences* **114**, 11285-11290 (2017).

19. M. Nosonovsky, V. Hejazi, Why superhydrophobic surfaces are not always icephobic. *ACS nano* **6**, 8488-8491 (2012).

20. Z. He, S. Xiao, H. Gao, J. He, Z. Zhang, Multiscale crack initiator promoted super-low ice adhesion surfaces. *Soft Matter* **13**, 6562-6568 (2017).

21. P. Guo *et al.*, Icephobic/anti‐icing properties of micro/nanostructured surfaces. *Advanced Materials* **24**, 2642-2648 (2012).

22. J. Lv, Y. Song, L. Jiang, J. Wang, Bio-inspired strategies for anti-icing. *ACS nano* **8**, 3152-3169 (2014).

23. Z. He, Y. Zhuo, F. Wang, J. He, Z. Zhang, Design and preparation of icephobic PDMS-based coatings by introducing an aqueous lubricating layer and macro-crack initiators at the ice-substrate interface. *Progress in Organic Coatings* **147**, 105737 (2020).

24. F. Wang, W. Ding, J. He, Z. Zhang, Phase transition enabled durable anti-icing surfaces and its DIY design. *Chemical Engineering Journal* **360**, 243-249 (2019).

25. A. Dhyani *et al.*, Facilitating Large‐Scale Snow Shedding from In‐Field Solar Arrays using Icephobic Surfaces with Low‐Interfacial Toughness. *Advanced Materials Technologies*, 2101032 (2021).

26. M. Mohseni *et al.*, Quasicrystalline Coatings Exhibit Durable Low Interfacial Toughness with Ice. *ACS Applied Materials & Interfaces* **13**, 36517-36526 (2021).

27. A. Dhyani *et al.*, Design and applications of surfaces that control the accretion of matter. *Science* **373**, eaba5010 (2021).

28. Li Q, Guo Z. Fundamentals of icing and common strategies for designing biomimetic anti-icing surfaces. *Journal of Materials Chemistry A* **6**, 13549-13581 (2018).

29. Y. Ru, R. Fang, Z. Gu, L. Jiang, M. Liu, Reversibly Thermosecreting Organogels with Switchable Lubrication and Anti‐Icing Performance. *Angewandte Chemie International Edition* **59**, 11876-11880 (2020).

30. Q. Rao, J. Zhang, X. Zhan, F. Chen, Q. Zhang, UV-driven self-replenishing slippery surfaces with programmable droplet-guiding pathways. *Journal of Materials Chemistry A* **8**, 2481-2489 (2020).

31. P. Irajizad, M. Hasnain, N. Farokhnia, S. M. Sajadi, H. Ghasemi, Magnetic slippery extreme icephobic surfaces. *Nature communications* **7**, 1-7 (2016).

32. K. Alasvand Zarasvand *et al.*, Metallic Plate Buckling As a Low Adhesion Mechanism for Durable and Scalable Icephobic Surface Design. *Advanced Materials Interfaces*, 2101402 (2021).

33. M. Liu, S. Wang, Z. Wei, Y. Song, L. Jiang, Bioinspired design of a superoleophobic and low adhesive water/solid interface. *Advanced Materials* **21**, 665-669 (2009).

34. G. Li *et al.*, Fish scale inspired design of underwater superoleophobic microcone arrays by sucrose solution assisted femtosecond laser irradiation for multifunctional liquid manipulation. *Journal of Materials Chemistry A* **3**, 18675-18683 (2015).

35. S. Xiao, B. H. Skallerud, F. Wang, Z. Zhang, J. He, Enabling sequential rupture for lowering atomistic ice adhesion. *Nanoscale* **11**, 16262-16269 (2019).

36. T. Ikoma, H. Kobayashi, J. Tanaka, D. Walsh, S. Mann, Microstructure, mechanical, and biomimetic properties of fish scales from Pagrus major. *Journal of structural biology* **142**, 327-333 (2003).

37. X. Li, B. Bhushan, A review of nanoindentation continuous stiffness measurement technique and its applications. *Materials characterization* **48**, 11-36 (2002).

38. R. Dou *et al.*, Anti-icing coating with an aqueous lubricating layer. *ACS applied materials & interfaces* **6**, 6998-7003 (2014).

39. N. D. Mulherin, R. B. Haehnel, Ice engineering: progress in evaluating surface coatings for icing control at corps hydraulic structures, *ENGINEER RESEARCH AND DEVELOPMENT CENTER HANOVER NH COLD REGIONS RESEARCH AND ENGINEERING LAB*, 2003.

40. Y. Zhuo *et al.*, Enhancing the mechanical durability of icephobic surfaces by introducing autonomous self-healing function. *ACS applied materials & interfaces* **10**, 11972-11978 (2018).

41. K. Kendall, Thin-film peeling-the elastic term. *Journal of Physics D: Applied Physics* **8**, 1449 (1975).